VOLUME 44 • NUMBER 2 • JANUARY 15, 2006

PUBLISHED IN 2 PARTS

ISSN 0887-624X

Articles published online in Wiley InterScience,
30 November 2005 through 8 December 2005

JOURNAL OF POLYMER SCIENCE

PART • A

Polymer Chemistry

Simultaneous Imaging

Supramolecular Nanostructure formed by a Coupling of π-Conjugated Polymer Chains

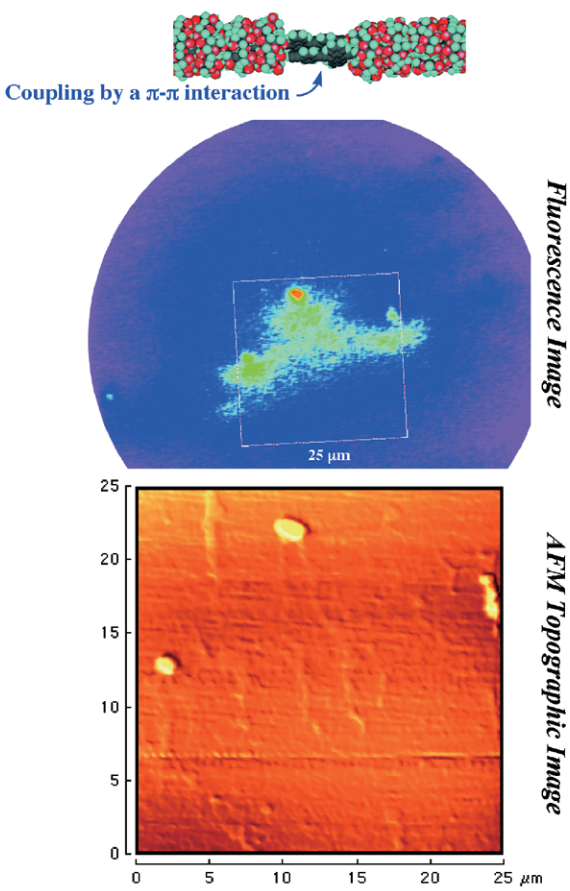

Long-Range Optical Communication via an Intertwined Network in the Near-Field

Simultaneous Imaging of the Structure and Fluorescence of a Supramolecular Nanostructure Formed by the Coupling of π-Conjugated Polymer Chains in the Intermolecular Interaction

KEN-ICHI SHINOHARA,[1,2] TASUKU SUZUKI,[2] TAKESHI KITAMI,[1] SHINGO YAMAGUCHI[2]

[1]School of Materials Science, Japan Advanced Institute of Science and Technology, 1-1 Asahidai, Nomi, Ishikawa 923-1292, Japan

[2]Graduate School of Engineering and Center for Interdisciplinary Research, Tohoku University, Aoba-yama, Aoba, Sendai 980-8578, Japan

Received 12 April 2005; accepted 1 October 2005
DOI: 10.1002/pola.21175
Published online in Wiley InterScience (www.interscience.wiley.com).

ABSTRACT: We fabricated a micrometer-long supramolecular chain in which π-conjugated polyrotaxane was coupled. A new experimental setup was designed and constructed, and the simultaneous direct imaging of the structure and fluorescent function was achieved. Furthermore, we identified the formation of a polymer intertwined network and observed novel fluorescence due to a long-range interaction via this intertwined network over a distance of 5 μm or more without quenching over 15 min in the near field. © 2005 Wiley Periodicals, Inc. J Polym Sci Part A: Polym Chem 44: 801–809, 2006

Keywords: atomic force microscopy (AFM); conjugated polymers; fluorescence; nanostructure; near-field; simultaneous imaging; polyrotaxane

INTRODUCTION

Polymers are very useful materials that display many excellent properties, and they have become indispensable in maintaining and developing our current way of life. In particular, π-conjugated polymers are recognized as being part of the next generation of functional polymers for optical and electronic applications.[1–3] Nevertheless, it is difficult to discuss the correlation between their structures and functions on a molecular level because these are diverse and dynamic and can be very complex. If the structure and functions of a polymer could be directly observed, with minimal inference or hypotheses, the relationship between the polymer structures and functions could be clarified. Consequently, molecular devices of a polymer might be created on the basis of new design concepts and new working principles.

Recently, we achieved the direct measurement of the chiral structure of single molecules in a π-conjugated helical polymer at room temperature with scanning tunneling microscopy[4] and atomic force microscopy (AFM).[5] On the other hand, as an example of single-molecule fluorescent detection, the imaging of single protein molecules with fluorescence microscopy has made remarkable progress since the development of single-fluorophore imaging methods, which have been used on air-dried surfaces.[6] Single fluorophores in aqueous solutions have been imaged with total internal reflection fluorescence microscopy

Correspondence to: K. Shinohara (E-mail: shinoken@jaist.ac.jp)

Journal of Polymer Science: Part A: Polymer Chemistry, Vol. 44, 801–809 (2006)

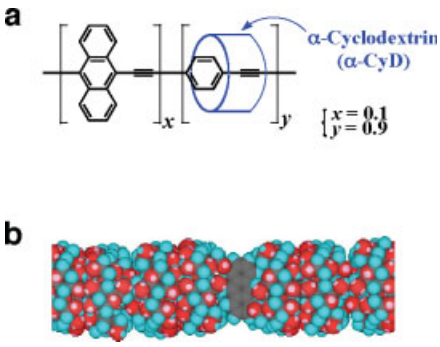

Figure 1. (a) Chemical structure of the polyrotaxane (+)-poly[AEPE-*rotaxa*-(α-CyD)] and (b) part of a molecular mechanics calculation optimized model of a polymer.

(TIRFM), in which the background fluorescence is significantly reduced[7] when a laser beam is totally reflected in the interface between the glass surface and solution; illumination is limited to only the vicinity near the glass surface. In our previous study, this single-molecule imaging method was expanded to an organic polymer solution system for the direct observation of single molecules of a photonic, functional, rigid–rodlike π-conjugated polymer.[8] In this study, we succeeded in the simultaneous imaging of the structure and fluorescent function of a π-conjugated polymer. Figure 1(a,b) shows the chemical structure and molecular model of a π-conjugated polyrotaxane, (+)-poly[(9,10-anthracenediyl-ethynylene-1,4-phenylene-ethynylene)-*rotaxa*-(α-cyclodextrin)] {(+)-poly[AEPE-*rotaxa*-(α-CyD)]}, that we synthesized in this study. Figure 2 shows a schematic view and an exterior view of the experimental setup that we built to simultaneously observe the structure and functions of the polymer on a molecular level, respectively. The setup consists of an AFM instrument[5,9] set above a substrate on which the specimen is mounted and an objective-type TIRFM[10] set below the substrate in air at room temperature. The AFM instrument can image the structure of the polymer on a molecular level, and the TIRFM instrument is able to image the fluorescence of the polymer at a video rate, so both the structure and fluorescent function of the polymer can be simultaneously imaged at the substrate surface.

EXPERIMENTAL

Microscopy

The TIRFM instrument was self-made by the modification of an inverted fluorescent microscope (Infinity optical system IX70, Olympus, Japan), as shown in Figure 2. An objective lens [60×, oil TIRFM, numerical aperture (NA) = 1.45; PlanApo, Olympus] of a high NA was attached to this TIRFM instrument. A laser beam from a helium-cadmium (He-Cd) laser [wavelength = 441.6 nm, 70 mW, continuous wave (CW), linearly polarized, blue laser; model Liconix M.4.70, Melles Griot, United States] was attenuated by neutral density filters (transmission = 21%) and focal expanded by a lens (LBE-3, Sigma Koki, Japan). The laser beam was focused by a lens (Focal length = 350 mm) on the back focal plane of the objective lens with an NA of 1.45. θ_a (66.6°) is the angle corresponding to NA (1.58 sin θ_a = NA; 1.58 is the refractive index of mica). The laser beam was reflected by a dichroic mirror (DM455, Olympus). θ_c (39.3°) is the critical angle of the mica–air interface (1.00 sin 90° = 1.58 sin θ_c; 1.00 is the refractive index of air). When the incident beam was positioned to propagate along the objective edge between θ_a and θ_c, the beam was totally internally reflected, producing an evanescent field at the mica–air interface (the 1/*e* penetration depth was ca. 40 nm at an angle

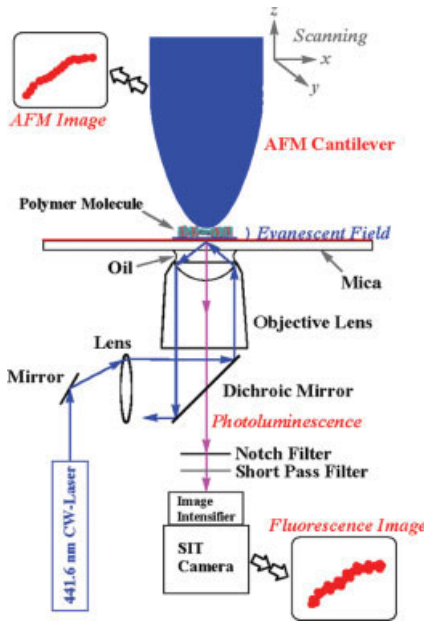

Figure 2. Experimental setup of the AFM–TIRFM instrument that the authors built to simultaneously observe the structure and functions of a polymer (not to scale). The notch filter is used to block incident light (441.6 nm). The short pass filter is used to cut the laser (670 nm) from the AFM detection system (see the Experimental section for details).

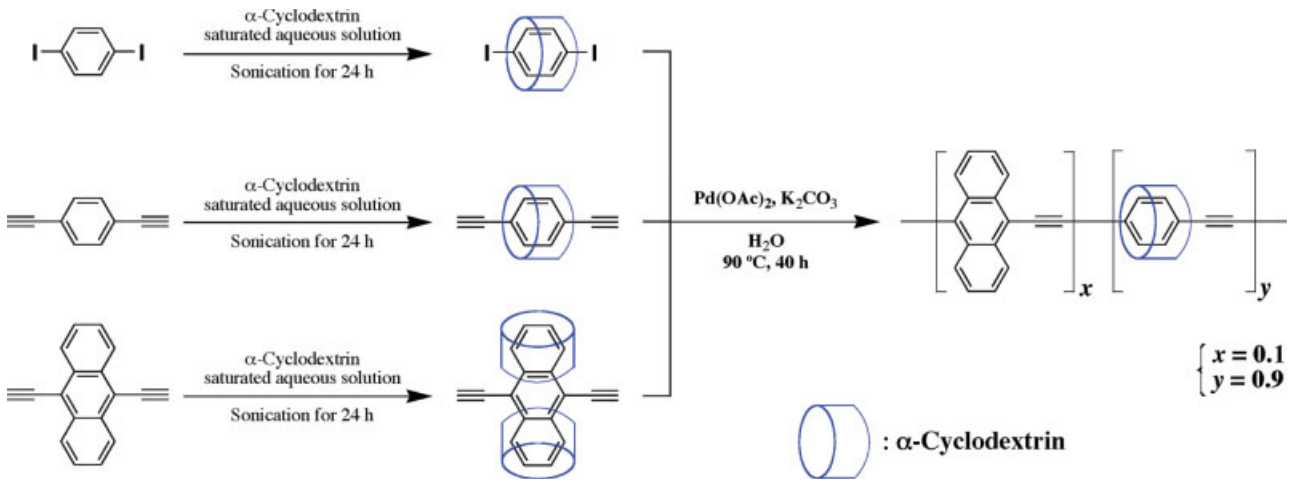

Scheme 1. Synthetic route of (+)-poly[AEPE-*rotaxa*-(α-CyD)] (see the Experimental section for the details).

of 60°). A mica film with a thickness of about 20 μm was used as the substrate.

The background of scattered light was rejected with a holographic notch filter (HNPF-441.6–1.0, Kaiser Optical System, United States), whose optical density at 441.6 nm was larger than 6. The scattered light (wavelength = 670 nm) from an AFM detection system was reduced with two short pass filters (cutoff wavelength = 630 nm). An intermediate image formed by spherical achromatic lenses (focal length = 100 mm) was enlarged by a projection lens (PE 5x, Olympus).

Nonfluorescent immersion oil (for ordinary use, (refractive index (n_d) = 1.516; Olympus) is suitable for single-molecule fluorescence imaging because it emits low fluorescence and has adequate viscosity.

Images were recorded with an silicon intensified target (SIT) camera (C1000 Type 12, Hamamatsu Photonics, Japan) coupled to an image intensifier (VS4-1845, Video Scope, United States) and stored on S-VHS videotape. Videotaped images were processed with a digital image processor (Argus-20, Hamamatsu Photonics).

Probe-scan-type AFM (PicoSPM, Molecular Imaging Corp., United States) was used in the contact mode with a soft cantilever [BL-RC150V (BioLever), Olympus] having a spring constant of 6 pN/nm. The pressure of tip contact was set as low as possible for the imaging of a soft contact. This probe-scan-type AFM instrument was combined with an objective-type TIRFM instrument, as stated previously (see Fig. 2). To image simultaneously by AFM and TIRFM, a sample on a stage with an AFM head was set to the TIRFM instrument. First, the TIRFM instrument was focused on a sample surface. Next, the AFM instrument was brought to the sample surface. The best imaging conditions were optimized under the observation of both images.

The AFM instrument (JSPM-4210, JEOL, Japan) was also used in a noncontact mode. A cantilever (OMCL-AC160TS, Olympus) with a resonant frequency of 300 kHz and a spring constant of 42 N/m was used. A high vacuum of 1×10^{-3} Pa was used, and the cantilever was oscillated with constant amplitude at room temperature. Imaging in a noncontact mode was carried out by the scanning of the probe while a frequency shift of −15 Hz was maintained.

Sample Preparation

A series of specimens were prepared with the spin-casting process on a clean bench (described later) for observation under the microscope. A polymer was dissolved in purified water at room temperature in air at atmospheric pressure, and a 3×10^{-4} mol/L concentration solution was prepared. A mica surface was cleaved and was spun with a rotation speed of 1×10^{3} rpm (17 Hz). With the cleaved surface exposed and rotated in this way, the polymer solution (10 μL) was cast onto the center of rotation of the surface, and the cast solution was left to dry at room temperature in atmospheric air. The prepared surface was then observed under the microscope.

Polymer Synthesis

As shown in Scheme 1, to prepare (+)-poly[AEPE-*rotaxa*-(α-CyD)], *p*-diiodobenzene (0.746 mmol,

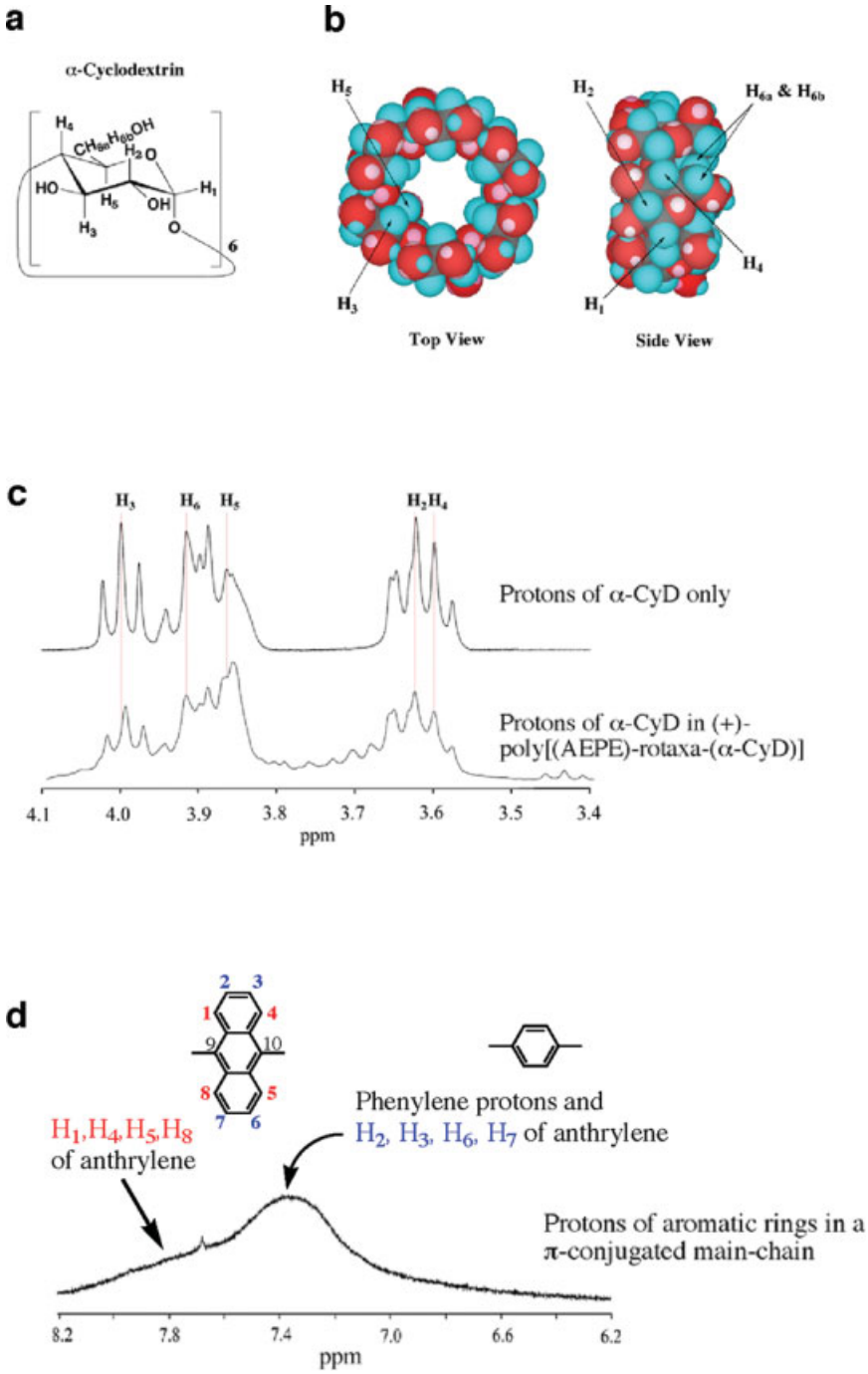

Figure 3. (a) Chemical structure of α-CyD, (b) molecular mechanics calculation optimized model of α-CyD, (c) 400-MHz ^{1}H NMR spectra of the polymer; (+)-poly [AEPE-*rotaxa*-(α-CyD)] and α-CyD in D_2O at 300 K (the external standard was TSP-d_4), and (d) aromatic region of (+)-poly[AEPE-*rotaxa*-(α-CyD)].

246 mg), *p*-diethynylbenzene (0.667 mmol, 84.0 mg), and 9,10-diethynylanthracene (7.39×10^{-2} mmol, 16.7 mg) were added to a saturated α-cyclodextrin (α-CyD) aqueous solution (149 mmol/L, 145 g/L) and irradiated with an ultrasonic wave to form the inclusion complexes [see Fig. 3(a,b) for the α-CyD ring structure]. These inclusion complexes were polymerized at 90 °C for 40 h with a palladium(II) acetate (8.73×10^{-2} mmol, 19.6 mg) and potassium carbonate (11.3 mmol, 1.56 g) catalyst system[11] to form

a polymer from the constituent complex monomers. After the polymerization reaction, the water-soluble and high-molecular-weight part was isolated by gel filtration and reprecipitation from an aqueous solution into methanol. The water-soluble (+)-poly[AEPE-*rotaxa*-(α-CyD)] was a dark-brown solid.

Polymerization yield: 220 mg (0.223 mmol). $[\alpha]_D^{20}$: +24.6° (c = 0.100, H_2O). Ultraviolet–visible (UV–vis): λ_{max} = 197 nm ($\varepsilon = 6.92 \times 10^3$), λ_{max} = 260 nm ($\varepsilon = 3.55 \times 10^3$), cutoff wavelength = 640 nm ($\varepsilon < 50$). Gel permeation chromatography (GPC): weight-average molecular weight = 1.47×10^6, weight-average molecular weight/number-average molecular weight (polydispersity index) = 2.3.

A GPC column (TSKgel α-M, Tosoh, Japan) with a high exclusion limit [poly(ethylene oxide), number-average molecular weight > 1×10^7] was used with an eluent of water at 40 °C. In addition, the threaded cyclodextrin on an anthracene unit was removed during the process for the purification.

In the ^{1}H NMR spectrum of the polymer in D_2O, the peaks at 5.1 and 4.0–3.6 ppm were assigned to the protons in α-CyD [see Fig. 3(c)]. A broad shoulder peak at 7.8 ppm was assigned to the 1-, 4-, 5-, and 8-position protons in the anthracene ring, and a broad peak at 7.4 ppm was assigned to the 2-, 3-, 6-, and 7-position protons in the anthracene and phenyl rings [see Fig. 3(d)].

RESULTS AND DISCUSSION

The π-conjugated polymer that we synthesized, (+)-poly[AEPE-*rotaxa*-(α-CyD)], in which cyclic molecules (α-CyD) are threaded onto a π-conjugated main chain, is shown in Figure 1(a,b). Thus, (+)-poly[AEPE-*rotaxa*-(α-CyD)] is a kind of polyrotaxane.[12,13]

If substituents such as long-chain alkyl groups are not bonded onto the main chains of a π-conjugated polymer, the polymer chains can interact with each other by π–π interactions, and π stacking occurs, causing aggregates to form; as a result, the solubility markedly decreases for any solvent. This poses a significant difficulty to overcome in the study of the molecular characterization of polymers at the single-molecule level. The use of a polyrotaxane in this study is based on our conjecture that cyclic molecules can physically block π stacking. Consequently, the solubility of such a π-conjugated polymer could be increased [see Fig. 1(b)]. In ^{1}H NMR measurements (see Fig. 3), 3-(trimethylsilyl)propionic-2,2,3,3-d_4 acid sodium salt (TSP-d_4; 98 atom % D; Isotec, Inc., Ohio) was used as an external standard. A capillary (a thin glass tube) enclosed a D_2O solution, and it was used for the measurement to prevent the inclusion of a TSP-d_4 molecule in an α-CyD hole.

The results of the ^{1}H NMR measurement of (+)-poly[AEPE-*rotaxa*-(α-CyD)] and α-CyD in D_2O are shown in Figure 3(c). Here, H_3 and H_5 protons face toward the inside of the α-CyD holes [see Fig. 3(b)]. Compared with those of polyrotaxane and α-CyD, the chemical-shift values of the H_3 and H_5 protons changed more noticeably than those of the other protons (H_2, H_4, and H_6). Here, the protons of H_2, H_4, and H_6 face toward the outside of the α-CyD holes. This significant change shows the formation of an inclusion complex.[14] Broad peaks in the lower magnetic field were assigned to the protons of the aromatic rings in the main chains of the π-conjugated polymer. A copolymerization ratio was calculated from the analytical results of the aromatic protons and α-CyD protons in a ^{1}H NMR spectrum. In addition, the molecular weight is greater than 10^6 g/mol, as measured by GPC with water as the eluent [see Fig. 4(a)], and the UV–vis absorption spectrum of this polymer in water shows that the absorption shifted significantly toward the longer wavelengths in comparison with the complex monomers, as far as 640 nm at the cutoff wavelength [$\varepsilon < 50$; see Fig. 4(b)]. It was concluded that the π-conjugated system had been expanded on the main chain. We determined from the results of the measurements that (+)-poly[AEPE-*rotaxa*-(α-CyD)] had been successfully synthesized. Furthermore, this polymer emitted fluorescence having a peak wavelength of 520 nm when excited at 442 nm in water [see Fig. 4(c)], which is the excitation light wavelength (441.6-nm CW laser) of TIRFM. This shows that (+)-poly[AEPE-*rotaxa*-(α-CyD)] can be observed with TIRFM imaging.

Figure 5(a) is a noncontact-mode AFM image of polymer chains extended outwards from a molecular globule. These chains were measured to be a micrometer-long structure. This is a new finding for a macromolecular structure. Figure 5(b) is a proposed model structure of a polyrotaxane. This model shows that the size of a single molecule is 1.5 nm. The height of a molecular globule was about 4 nm, as shown in Figure 5(c); this

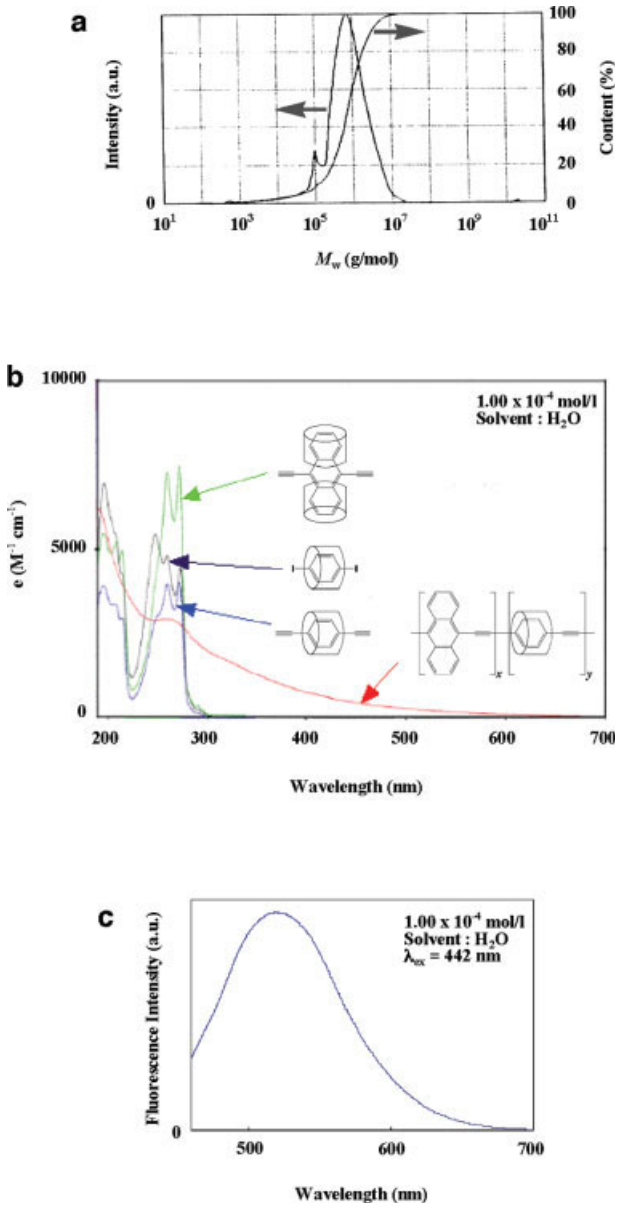

Figure 4. (a) GPC chart of a polymer at 40 °C (UV detector was used, and the wavelength was 190 nm; see the Experimental section for details), (b) UV–vis spectra of a polymer and monomers in H_2O at room temperature, and (c) photoluminescence spectrum of a polymer in H_2O at room temperature.

was height of three molecules. Each chain that extended outward from a globule was a single molecular size, as shown in Figure 5(d). Although a micrometer-long chain was observed directly in an AFM measurement, the long polymer chain could not be synthesized by a cross-coupling reaction[11] in this study. Hence, we thought that π-conjugated polyrotaxane chains a nanometer long coupled to form a micrometer-long supramolecular chain because of an intermolecular interaction at the chain ends like a train on a nanometer scale, as shown in Figure 5(b). Actually, a number of short substances a nanometer long were observed in line when imaged by AFM at the other large area, which had a height of a single molecular size of 1.5 nm. Therefore, we thought that these short substances were the chains of (+)-poly[AEPE-*rotaxa*-(α-CyD)] without an intermolecular interaction. It is a very interesting and new finding that the polymer chains formed a micrometer-long coupling supramolecular structure by a self-assembly event without forming a disordered aggregate.

Figure 5(e) is a contact-mode AFM image of the intertwined network of the polymer chains. The cross sections of these polymer strands were analyzed, and the height of each polymer strand was found to be about 1 nm, as shown in Figure 5(f). This value is less than 1.5 nm, which is the external diameter of α-CyD in a single polyrotaxane chain; a molecular mechanics (MM2) calculated optimized model is shown in Figure 5(b). However, it should not be considered the actual value because α-CyD threaded onto a polymer chain is squeezed down and deformed by contact pressure from the probe with the cantilever. Therefore, we concluded that the strands of a π-conjugated polymer had been observed on a single-molecule level. It was determined from these observations that each spot in the AFM image consisted of a molecular globule in which the polymer chains were intertwined like a wound-up ball of string and that the stranded polymer chains extended outwards from these globules, just as a string can come loose from a ball when it is unwound, as shown in Figure 5(g).

Figure 6 shows the results of the simultaneous imaging of the structure and the fluorescent function of the π-conjugated polymer. The position of the brightest spots in the TIRFM image shown in Figure 6(a) matches the position of the highest spots in the AFM image shown in Figure 6(b). This indicates that simultaneous direct imaging is successful with this AFM–TIRFM setup and that some high spots emit a strong fluorescence. In Figure 6(c,d) (control experiments), no fluorescent and no absorbate can be observed on a mica substrate, and it is also shown that the simultaneous imaging of a π-conjugated polymer is successful. In Figure 6(a), a relatively weak fluorescence can also be observed in the region around the three very

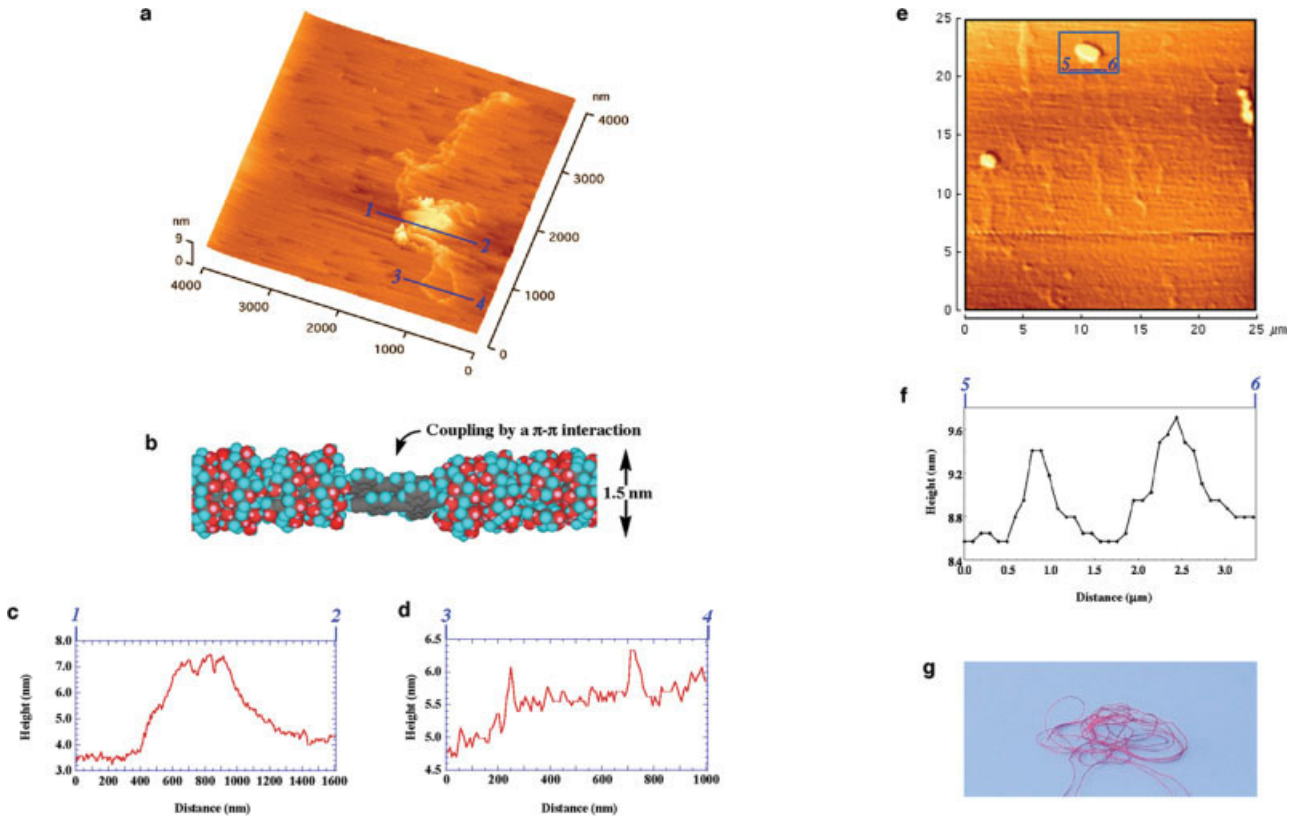

Figure 5. (a) Noncontact-mode AFM image of single chains from a molecular globule of (+)-poly[AEPE-*rotaxa*-(α-CyD)] on mica at room temperature (a high vacuum of 1×10^{-3} Pa was used, and the cantilever was oscillated with a constant amplitude at room temperature; imaging in a noncontact mode was carried out by the scanning of the probe while a frequency shift of −15 Hz was maintained), (b) proposed model of the polymer coupling by π–π interaction at the chain ends, (c) analytical result of a cross section of the line from 1 to 2 indicated in the AFM image of part a, (d) cross-sectional analysis of the line from 3 to 4 indicated in the AFM image of part a, (e) contact-mode AFM image of the intertwined network as a nanostructure, (f) analytical result of a cross section of the line from 5 to 6 indicated in the AFM image of part e, and (g) string model of the polymer chains in the region shown in the square in the AFM image of part e.

bright spots. In the case of TIRFM, which is optical microscopy, there is an absolute limit to the image resolution. With AFM, however, some stringlike objects that are deemed to be aggregated polymer chains on a molecular level can be observed in the identical area in which the formation of a nanostructured network by the loose connection of the assembled π-conjugated polymer chains can also be observed, as shown in Figure 6(b). Therefore, the TIRFM image shown in Figure 6(a) verifies that the light emitted from the brightest spots and their surrounding area is the fluorescent light emitted by the polymer. In addition, bleaching was only slightly observed over 15 min during the imaging. The polymer strands were extended from the highest spot, which was the molecular globule of a π-conjugated polymer, in the AFM image, as shown in Figure 6(b).

It is most interesting to note that the fluorescence is brighter in the area formed by the connection of the three brightest spots, as shown in the TIRFM image in Figure 6(a). This is the fluorescence due to a long-range interaction of a π-conjugated polymer and the protons. The molecular globules have many π electrons in an excitation state (π* state) and an excitation energy transfer via a loosely connected π-conjugated polymer intertwined network as a nanostructure. We think that the fluorescence is a light

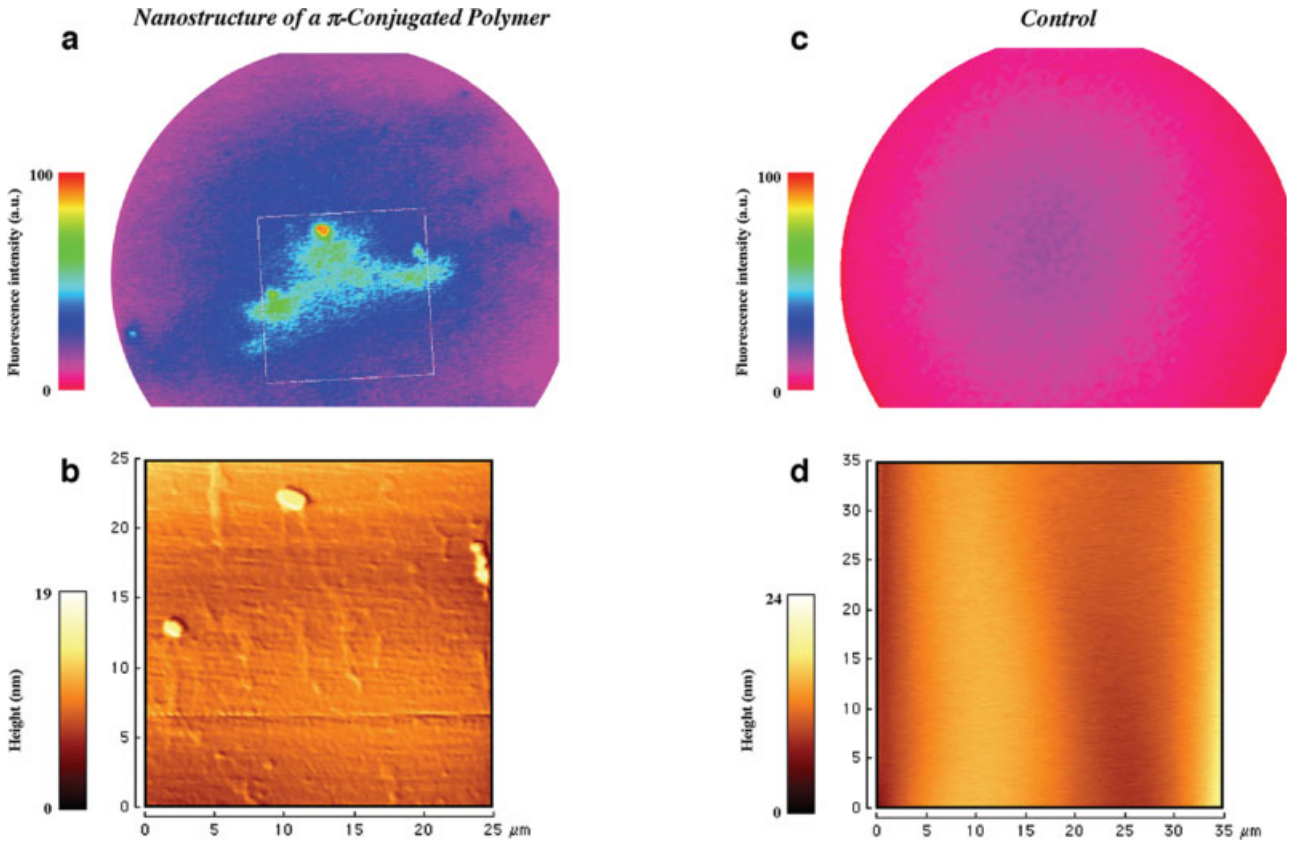

Figure 6. Simultaneous imaging by TIRFM and AFM of the intertwined network, that is, the nanostructure of (+)-poly[AEPE-*rotaxa*-(α-CyD)] on mica in air at room temperature: (a) a fluorescent image observed by TIRFM in which the inset with a square size of 25 μm $\times$ 25 μm was imaged by AFM (the excitation wavelength was 441.6 nm with a CW He-Cd laser, and the observed fluorescence wavelength was over 475 nm; see the Experimental section for the details), (b) a topographic image observed by contact-mode AFM with an area of 25 μm $\times$ 25 μm in which the central part was observed by TIRFM, (c) a fluorescent image of the mica substrate as a control experiment of TIRFM imaging, and (d) a topographic image of the surface of the mica substrate as a control experiment of AFM imaging with an imaging area of 35 μm $\times$ 35 μm.

emission based on not only the combined phenomena of energy migration,[15] energy transfer, and energy hopping between many chromophores but also an effect of the total internal reflection: thus, the photons in the direction of a wave number vector of the Goos-Hänschen shift in the total internal reflection that scattered at the molecular globules of a π-conjugated polymer. Surprisingly, the photons propagated to a π-conjugated polymer intertwined network over a distance of 5 μm or more. As the result, the fluorescence was brighter in the area. In other words, this phenomenon can be considered optical communication over a long range. This novel phenomenon suggests the possibility of using the polymers to create an intertwined molecular network device in the future. As a new chemistry, it is worthwhile that the relationship of the structure and function can be directly discussed on a molecular level.

The authors thank Prof. Dr. Hideo Higuchi at Tohoku University for his useful technical advice. This research was financially supported by Grants-in-Aid for Scientific Research for Young Scientists (A) from the Ministry of Education, Culture, Sports, Science, and Technology (MEXT) of Japan (no. 15685007) and the System Development Program for Advanced Measurement and Analysis (SENTAN) from the Japan Science and Technology Agency (JST) (to K. Shinohara).

REFERENCES AND NOTES

1. Martin, R. E.; Diederich, F. Angew Chem Int Ed Engl 1999, 38, 1350.
2. Meier, H. Angew Chem Int Ed Engl 1992, 31, 1399.
3. Bleier, H. Organic Materials for Photonics; Elsevier: Amsterdam, 1993; p 77.
4. Shinohara, K.; Yasuda, S.; Kato, G.; Fujita, M.; Shigekawa, H. J Am Chem Soc 2001, 123, 3619–3620, Editors' choice, Science 2001, 292, 15.
5. Shinohara, K.; Kitami, T.; Nakamae, K. J Polym Sci Part A: Polym Chem 2004, 42, 3930.
6. Trautman, J. K.; Macklin, J. J.; Brus, L. E.; Betzig, E. Nature 1994, 369, 40.
7. Funatsu, T.; Harada, Y.; Tokunaga, M.; Saito, K.; Yanagida, T. Nature 1995, 374, 555.
8. Shinohara, K.; Yamaguchi, S.; Wazawa, T. Polymer 2001, 42, 7915–7918.
9. Binning, G.; Quate, C. F.; Gerber, C. Phys Rev Lett 1986, 56, 930.
10. Tokunaga, M.; Kitamura, K.; Saito, K.; Hikikoshi-Iwane, A.; Yanagida, T. Biochem Biophys Res Commun 1997, 235, 47–53.
11. Bumagin, N. A.; More, P. G.; Beletskaya, I. P. J Organomet Chem 1989, 371, 397.
12. Harada, A.; Li, J.; Kamachi, M. Nature 1992, 356, 325–327.
13. Ohga, K.; Takashima, Y.; Takahashi, H.; Kawaguchi, Y.; Yamaguchi, H.; Harada, A. Macromolecules 2005, 38, 5897–5904.
14. Wood, D. J.; Hruska, F. E.; Saenger, W. J Am Chem Soc 1977, 99, 1735.
15. Grage, M. M.-L.; Wood, P. W.; Ruseckas, A.; Pullerits, T.; Mitchell, W.; Burn, P. L.; Samuel, I. D. W.; Sundström, V. J Chem Phys 2003, 118, 7644–7650.